Initial H_2O-induced Oxidation of Si(100)–(2×1)

Marcus K. Weldon, Boris B. Stefanov, Krishnan Raghavachari, and Y. J. Chabal

Bell Laboratories, Lucent Technologies, Murray Hill, New Jersey 07974

(Received 28 March 1997)

Surface infrared absorption spectroscopy and density functional cluster calculations are used to definitively demonstrate that the Si-Si dimer bond is the target for the initial insertion of oxygen into the Si(100)–(2×1) surface, following H_2O exposure and annealing. This reaction, in turn, facilitates the subsequent incorporation of O into the Si backbonds, thereby promoting (local) oxidation. [S0031-9007(97)04218-X]

The oxidation of silicon has been the subject of intense scientific and technological interest due to the ubiquitous use of thin oxide films as insulating layers in microelectronic devices. While great strides have been made in understanding the bulk properties of these oxide layers, much remains to be understood about the formation and thermal evolution of the Si/SiO_2 interface [1]. Specifically, the structure, composition, and even thickness of the so-called "transition region" between the termination of the bulk silicon and the overlying stoichiometric oxide layer is highly contentious [1]. Furthermore, the device dimensions have now decreased to the point where one monolayer may represent as much as ~33% of the total thickness of the (gate) oxide layer, so that characterizing and controlling the uniformity of the Si/SiO_2 interface is of paramount importance. In order to understand the growth of such interfaces, we have developed a combined experimental and theoretical approach that not only uncovers the microscopic phenomena specific to Si oxidation, but can also be successfully applied to a wide range of problems in semiconductor surface chemistry.

The initial focus of our investigation is the thermal evolution of water-exposed Si(100), as a precursor to understanding the wider oxidation process. The H_2O:Si(100) system has received considerable attention [2,3] due to its apparent simplicity and the widespread use of H_2O in industrial oxidation processes. Early conflicting reports have focused on the nature of the adsorption (now established to be predominantly dissociative, forming SiH and SiOH) [2]. However, little is known about the decomposition of these hydroxyl species upon annealing to higher temperatures due to the complexity of the initial oxidation process, which necessitates both the use of high resolution experimental probes with submonolayer sensitivity and accurate theoretical modeling of the many different structural possibilities.

We have devised a novel experimental geometry that enables direct observation of the vibrations of all species relevant to this complex system (SiO, SiH, and SiOH) with high spectral resolution. In order to correctly interpret the IR data, we have also employed a gradient-corrected density functional method on embedded cluster models. This methodology permits accurate evaluation of both the relative energetics and the characteristic frequencies of the various surface oxide structures, thereby allowing the *unambiguous* characterization of the inherently inhomogeneous initial oxidation process.

This work shows that the homogeneous H_2O-exposed surface (comprising one H and one OH per dimer) evolves into a mixed phase consisting of oxygen-free, and singly and doubly oxidized dimer units. Furthermore, we identify two distinct intermediate Si-O species at 675 K that demonstrate that oxidation starts with the insertion of an oxygen into the surface dimer bond, which facilitates subsequent incorporation of oxygen into the silicon backbonds.

The primary experimental advance is the development of a multiple internal reflection (MIR) geometry that utilizes short (1 cm) Si(100) samples (float zone, 10 Ω cm) and low data acquisition temperatures to probe the spectral region below 1500 cm^{-1}. While the IR throughput down to 900 cm^{-1} is sufficient to achieve the required sensitivity (using a total of 20 internal reflections) to both the parallel and perpendicular components, the data quality depends on precise temperature control (± 1 K) and elaborate schemes to reject externally reflected (stray) radiation [4]. The principal limitation of the MIR geometry is the reduced sensitivity to perpendicular vibrations, due to effective screening of the normal component of the electric field (see discussion) and the low frequency cutoff of ~850 cm^{-1}. Therefore, we also utilize Si(100) samples that have a buried metallic layer of $CoSi_2$ (that acts as an internal "mirror") providing sole sensitivity to vibrations normal to the surface [5], and increasing the spectral range down to 400 cm^{-1}, using a synchrotron IR source. The combination of both geometries yields a complete spectroscopic picture.

The sample is mounted in a UHV chamber (base pressure $<2 \times 10^{-10}$ torr) on a liquid nitrogen cold finger that permits cooling to ~100 K. Resistive heating using a four point electrical contact with current/temperature feedback allows temperature control to ± 1 K over the entire range (100–1200 K). The accuracy of the chromel/alumel thermocouple is ensured by careful calibration against the pyrometric temperature [4]. A double-directed doser allows simultaneous exposure of the front and back

surfaces of the sample. A nominal H_2O pressure rise of $\sim 1 \times 10^{-10}$ Torr for 10 s yields a saturation coverage at 175 K.

Infrared spectra were obtained after annealing the saturated Si(100) surface over the 300–1125 K range (in steps of as little as 10 K in the critical region between 550 and 700 K). Figure 1 summarizes the essential spectra observed after annealing to 300 and 675 K, respectively. After annealing to 300 K, a single SiH stretch mode at 2086 cm^{-1} (p)/2084 cm^{-1} (s) is observed, together with a single OH stretch at 3660 cm^{-1} and the related SiO mode at 840 cm^{-1} [Figs. 1(c) and 1(d)]. Notably, the absence of features in the 900–1300 cm^{-1} region indicates that no Si-O-Si species are formed at this temperature [Figs. 1(a) and 1(b)]. These observations are consistent with the known initial surface structure [3,6,7] with H and OH passivating the dangling bonds of the same dimer, HSi-SiOH [Fig. 2(a)]. The spectrum is completely unchanged after annealing to 575 K. However, substantial changes begin to occur in the 575 to 675 K temperature range, as all the above features disappear and eight new modes appear in the p-polarized spectra [Figs. 1(e)–1(h)]: five in the SiH stretching region (2090, 2099, 2109, 2117, and 2165 cm^{-1}) and three in the low frequency Si-O stretching region (993, 1013, and 1042 cm^{-1}). Importantly, all the features are relatively narrow and well defined, consistent with the formation of several discrete structures rather than a continuum of different Si-O and SiH species.

Partial information about the surface composition following the 675 K anneal can be deduced from the frequencies and polarizations of the SiH stretching modes [Fig. 1(g)]. The modes at 2090 and 2099 cm^{-1} can be definitively assigned to the asymmetric (ν_a: parallel polarized) and symmetric (ν_s: perpendicular polarized) stretching modes of a coupled monohydride species, HSi-SiH [6,8], providing clear evidence for the segregation of oxygen-free dimers. The mode at 2165 cm^{-1} can be accounted for only by insertion of oxygen into a Si backbond (O_xSi-H), as all the "pure" SiH_x stretching modes occur below 2150 cm^{-1} [9–11]. The origin of the two other modes at 2109 and 2117 cm^{-1}, previously assigned to Si dihydride [6,9], cannot in fact be unambiguously determined without analysis of the effect of oxygen incorporation (summary of experiment in Table I).

The critical spectral information is therefore contained in the low frequency region where all the SiO vibrations are known to occur. In this region, the three distinct modes observed (all occurring in a narrow, 50 cm^{-1} frequency interval) exhibit a distinct polarization: p:s intensity ratio of 1.0 ± 0.1 for each mode as measured using MIR [Fig. 1(f)], but are all undetectable [Fig. 1(e)] when using grazing incidence reflection ($CoSi_2$ samples with strict sensitivity to the normal component).

These observations are crucial to the correct assignment of the SiO modes, yet such information was unavailable in all previous vibrational studies of the water-induced oxidation process, due to limited spectral resolution or substrate inhomogeneities [9,10]. Furthermore, a detailed theoretical analysis of the relative energetics and vibrational frequencies, essential for an unequivocal characterization of the many possible SiO structures, has not previously been reported.

The starting point for our theoretical treatment is a Si_9 cluster fragment which has been successfully used to study various adsorption processes on Si(100)–(2×1) [7,8,12].
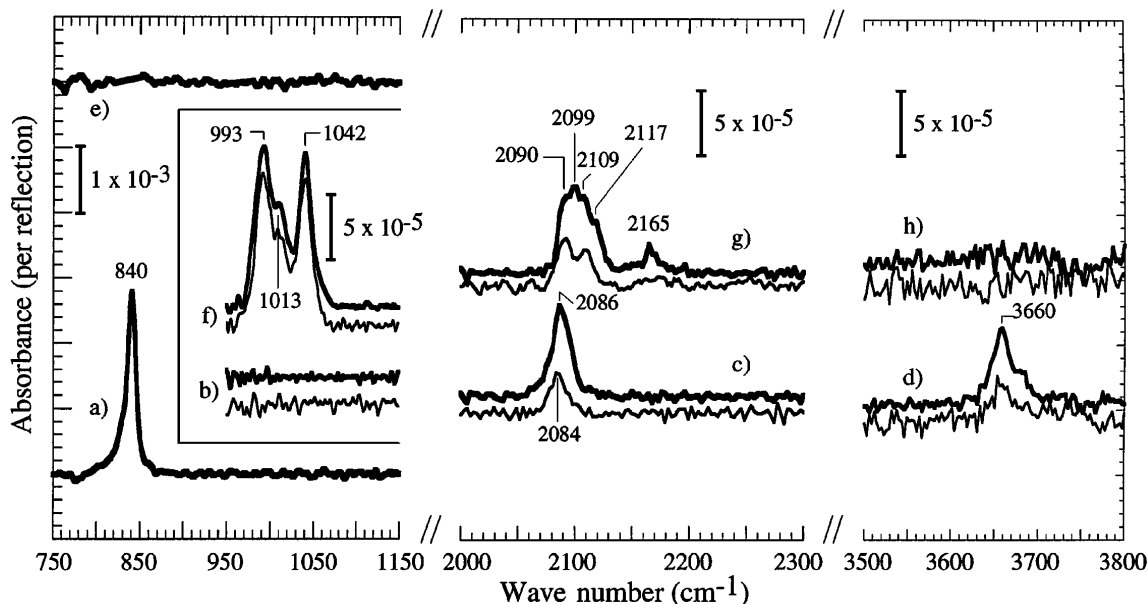
FIG. 1. IR spectra using p (—) and s (—) polarization for the H_2O-saturated Si(100)–(2×1) surface after annealing to 300 K (a)–(d) and 675 K (e)–(h). (b)–(d) and (f)–(h) were obtained using the short sample (45°) MIR geometry described in the text. (a) and (e) were acquired using the external reflection ($CoSi_2$) geometry and a synchrotron source. In (a) and (e) D_2O data shown for clarity.
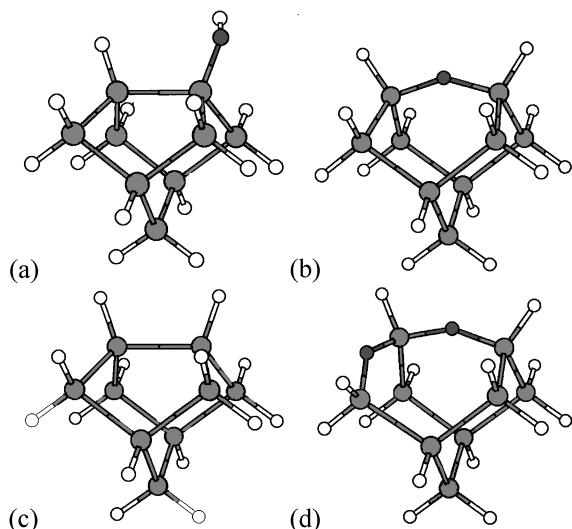
FIG. 2. Cluster models of Si(100)–(2×1) surface species identified in this work. Atoms are represented as follows: grey denotes Si, white denotes H, and black denotes O.

This cluster consists of a single dimer together with three underlying layers of atoms as shown in Fig. 2. The severed Si-Si bonds that connect this fragment with the rest of the surface are capped with H atoms to avoid artifacts that arise from unphysical excess of spin or charge. The initial state of the water-exposed surface is thus described by a $Si_9H_{13}OH$ [Fig. 2(a)] cluster with H_2O dissociatively adsorbed as H and OH onto the dimer Si atoms.

We have analyzed 15 distinct structures corresponding to insertion of a total of zero to five oxygen atoms into the surface Si-Si dimer bond and/or backbonds of our cluster. Additional boundary constraints are imposed to avoid unphysical relaxation in the model clusters: The first and second layer atoms as well as all adsorbate atoms are allowed to relax fully, while the third and fourth layer atoms are held fixed along ideal crystalline directions (Si-Si = 2.35 Å, Si-H = 1.48 Å). We use the well-documented B3LYP [13] gradient corrected density functional method with the polarized 6-31G** basis set for the first and second layer silicons as well as all the adsorbed atoms, and the 6-31G basis set for the remaining atoms

TABLE I. A summary of theoretical and experimental frequencies [cm^{-1}] of the structures shown in Fig. 2.

Mode	Structure	Theory [17]	Experiment
ν_a (Si-O)	HSi-O-SiH	993	993
ν_a'' (Si-O)	HSi-O-Si(O)H	1013	1013
ν_a' (Si-O)	HSi-O-Si(O)H	1046	1042
ν (Si-H)	HSi-SiOH	2084	2084
ν_a (Si-H)	HSi-SiH	2091	2090
ν_s (Si-H)	HSi-SiH	2098	2099
ν_a (OSi-H)	HSi-O-SiH	2110	2109
ν_s (OSi-H)	HSi-O-SiH	2113	2117
ν (OSi-H)	HSi-O-Si(O)H	2110	2109
ν (O$_2$Si-H)	HSi-O-Si(O)H	2158	2165

[14]. For each of the 15 structures, the relative positions of the nuclei are optimized to yield minimal energies subject to the above constraints.

Second-order differentiation of the minimal energies with respect to the nuclear coordinates yields force constants and the associated vibrational frequencies for each of the structures. The shifts and splittings in the vibrational frequencies caused by the differing local chemical environments in the different structures are accurately reproduced by the B3LYP method [15]. The computed harmonic frequencies are made directly comparable to the observed bands by a uniform frequency shift for each type of vibration, e.g., SiH stretch, SiO stretch, requiring the positive identification of only a single spectral band (Table I).

The 2084 cm^{-1} feature in the s-polarized 300 K spectrum [Fig. 1(c)] is an obvious choice for calibration of the computed frequencies in this spectral region. The observed frequencies at 2090 and 2099 cm^{-1} with s and p polarizations [Fig. 1(g)] are then in good agreement with the antisymmetric and symmetric SiH stretching modes of the unoxidized HSi-SiH species shown in Fig. 2(c) (theoretical values: 2091 and 2098 cm^{-1}) [16].

The remaining SiH stretches at 2109, 2117, and 2165 cm^{-1} clearly suggest incorporation of oxygen into the surface silicon framework. A careful analysis of the computed frequencies for multiply oxidized species precludes the presence of $[(O)_3Si\text{-}H]$ based on the absence of its characteristic absorption in the 2240–2280 cm^{-1} range. Such higher oxides are also ruled out since they possess distinct SiO bands around 1100 cm^{-1} [4]. Thus single and double oxygen inserted dimer sites are the only structural possibilities to account for the observed spectral features.

We find that oxygen insertion into the Si-Si dimer bond is clearly favored over backbond insertion. Thermodynamically, HSi-O-SiH species shown in Fig. 2(b) is 0.3 eV more stable than HSi-Si(O)H [17], consistent with the weaker nature of the strained dimer bond. In addition, it is likely that the dimer bond is more amenable to attack than the sterically more protected backbond. Thus both thermodynamic and kinetic factors clearly favor the initial formation of HSi-O-SiH. Notably, subsequent oxygen insertion always leads to an increase in the corresponding SiO asymmetric stretching frequency. Therefore we identify the dominant 993 cm^{-1} mode, the lowest observed frequency in this region, as the asymmetric SiO stretch of HSi-O-SiH, and shift the analogous theoretical frequencies accordingly. Importantly, this assignment of the HSi-O-SiH species is also consistent with additional features seen in the SiH stretching region. HSi-O-SiH has calculated antisymmetric and symmetric Si-H stretching frequencies (2110 and 2113 cm^{-1}) in good agreement with the experimentally observed s- and p-polarized modes (2109 and 2117 cm^{-1}) and their corresponding isotopic shifts upon deuteration. These observations definitively rule out the existence of a surface dihydride under these conditions [8].

The insertion of the first oxygen into the dimer bond immediately suggests the HSi-O-Si(O)H species shown in Fig. 2(d) as the likely structure for the doubly oxidized dimer. Indeed, the two coupled asymmetric SiO stretches in the doubly oxidized HSi-O-Si(O)H, predicted at 1013 and 1046 cm^{-1}, are in excellent agreement with the two remaining observed bands in this region, at 1013 and 1042 cm^{-1}, respectively. Again, the good correspondence between theory (2159 cm^{-1}) and experiment (2165 cm^{-1}) for the related O_2Si-H mode further supports this assignment [18]. Similar comparisons in the SiO and SiH regions rule out the presence of alternative doubly oxidized species such as HSi-Si(O)$_2$H. The observation of initial insertion of oxygen into the dimer bond is in direct contrast to previous work suggesting preferential insertion of oxygen into a backbond [9]. These earlier conclusions were based on the relative strength of the Si-Si dimer and backbonds for the clean Si(100)–(2×1) surface, without accounting for the reversal of the relative bond strengths that is predicted to occur upon adsorption.

Finally, the preceding assignments are compatible with the observed polarizations of the SiO modes. Importantly, in order to interpret the p:s polarization ratio, the effective dielectric function of the layer (ϵ) must first be determined, since the perpendicular absorption is screened (attenuated) by a factor of $|\epsilon|^{-2}$ relative to the parallel. If we take $\epsilon = 2.0$ [19], as established for an SiH layer above the surface plane, we find that the p:s ratio observed for the 993 and 1013 cm^{-1} modes is entirely consistent with the (projected) parallel orientation of these modes (90° and 82° to the surface normal [4], respectively). In contrast, the 1042 cm^{-1} mode is oriented 62° to the normal and should, therefore, exhibit a measurable perpendicular absorption and a corresponding p:s ratio >1.0 [4], if $\epsilon = 2.0$. However, the value of ϵ associated with this mode (SiO layer) should, in fact, be substantially greater than that for an SiH $over$layer, since the perpendicular motion arises from the Si-O-Si group that is embedded in the (high index) Si substrate. Indeed, we estimate a lower bound of $\epsilon \geq 2.6$ for this layer by reference to both MIR (p:$s = 1.0$) and external reflection data (absorption assumed to be less than or equal to the detection limit). Thus, the observed polarizations of all three SiO modes are in good agreement with the calculated values for the singly- and doubly-oxidized dimer structures, when the appropriate optical parameters are employed.

In summary, the combination of novel experimental techniques and accurate theoretical analysis allows definitive assignment of all observed spectroscopic features to a combination of HSi-SiH, HSi-O-SiH, and HSi-O-Si(O)H dimers that are formed during the initial stages of the water-induced oxidation of Si(100)–(2×1). Although subsequent annealing to higher temperatures leads to a surface that is significantly less homogeneous [4], preliminary results suggest that the state of the surface can likewise be understood by comparison of the observed frequencies with those predicted for a combination of higher order, three to five oxygen-containing clusters. Furthermore, we have found that the unique oxide structures observed after annealing the water-exposed Si(100)–(2×1) surface above 800 K are also characteristic of interfacial defect structures in a variety of technologically important oxide films. These observations clearly demonstrate that this approach holds tremendous promise for understanding the entire oxidation process at an unprecedented level. Moreover, it should also be $generally$ applicable to the study of systems with similarly localized (nanoscale) structural phenomena.

[1] *Proceedings of the 1st–3rd International Symposium on the Physics and Chemistry of SiO$_2$ and the Si/SiO$_2$ Interface,* edited by H. Z. Massoud, E. H. Poindexter, and C. R. Helms (Electrochem. Soc., Pennington, NJ, 1988–1996), Vol. 3.

[2] P. A. Thiel and T. E. Madey, Surf. Sci. Rep. **7**, 211 (1987); H. N. Waltenberg and J. T. Yates, Jr., Chem. Rev. **95**, 1589 (1995).

[3] L. M. Struck *et al.,* Surf. Sci. **380**, 444 (1997).

[4] A. B. Gurevich, M. K. Weldon, B. B. Stefanov, K. Raghavachari, and Y. J. Chabal, J. Chem. Phys. (to be published).

[5] Y. J. Chabal, M. A. Hines, and D. Feijoo, J. Vac. Sci. Technol. A **13**, 1719 (1995).

[6] Y. J. Chabal, Phys. Rev. B **29**, 3677 (1984).

[7] K. Raghavachari, Y. J. Chabal, and L. M. Struck, Chem. Phys. Lett. **252**, 230 (1996).

[8] Y. J. Chabal and K. Raghavachari, Phys. Rev. Lett. **53**, 282 (1984); **54**, 1055 (1985).

[9] H. A. Ibach, H. D. Bruchmann, and H. Wagner, Appl. Phys. A **29**, 113 (1982).

[10] P. Gupta, A. C. Dillon, A. S. Bracker, and S. M. George, Surf. Sci. **245**, 360 (1991); D. B. Mawhinney, J. A. Glass, Jr., and J. T. Yates, Jr., J. Phys. Chem. **101**, 1202 (1997).

[11] Y. J. Chabal, G. S. Higashi, K. Raghavachari, and V. A. Burrows, J. Vac. Sci. Technol. A **7**, 2104 (1989).

[12] R. Konecny and D. J. Doren, J. Chem. Phys. **106**, 2426 (1997).

[13] A. D. Becke, J. Chem. Phys. **98**, 5648 (1993); C. Lee, W. Yang, and R. G. Parr, Phys. Rev. B **37**, 785 (1988).

[14] W. J. Hehre, L. Radom, P. v. R. Schleyer, and J. A. Pople, *Ab Initio Molecular Orbital Theory* (J. Wiley, New York, 1986).

[15] G. Rauhut and P. Pulay, J. Phys. Chem. **99**, 3093 (1995).

[16] The computed frequencies have been shifted down uniformly by 102 cm^{-1} in the SiH stretch region and by 17 cm^{-1} in the SiO asymmetric stretch region.

[17] B. B. Stefanov and K. Raghavachari, Surf. Sci. Lett. (to be published).

[18] The OSi-H stretch of HSi-O-Si(O)H, calculated to be at 2110 cm^{-1}, also contributes to the absorption at 2109 cm^{-1}.

[19] P. Jakob and Y. J. Chabal, J. Chem. Phys. **95**, 2897 (1991).